Investigation of site-selective symmetries of Eu^{3+} ions in KPb_2Cl_5 by using optical spectroscopy

Concepción Cascales

Instituto de Ciencia de Materiales de Madrid, CSIC, Calle Sor Juana Inés de la Cruz, Cantoblanco, E-28049 Madrid, Spain

Joaquín Fernández, Rolindes Balda

Departamento Fisica Aplicada I, Escuela Superior de Ingenieros, Alda. Urquijo s/n 48013 Bilbao, Spain, and Unidad Física de Materiales CSIC-UPV/EHU and Donostia International Physics Center, Apartado 1072, 20080 San Sebastian, Spain
wupferoj@bi.ehu.es

Abstract: Site-selective time-resolved spectroscopy of Eu^{3+} in KPb_2Cl_5 has been investigated by using fluorescence line narrowing technique. A crystal field analysis and simulation of the experimental results has been performed in order to parametrize the crystal field at the Eu^{3+} sites. Three symmetry independent crystal field sites for the rare-earth ion in this crystal were found. A plausible argument about the crystallographic nature of these sites is given.

OCIS codes: (140.3380) Laser Materials; (300.6320) Spectroscopy, high resolution.

References and links

1. G.L. Vossler, C.L. Brooks, and K.A. Winik, "Planar Er:Yb glass ion exchanged waveguide laser," Electron. Lett. **31**, 1162-1163 (1995).
2. T.H. Whitley, C.A. Millar, R. Wyatt, M.C. Brierley, and D. Szebesta, "Upconversion pumped green lasing in erbium doped fluorozirconate fibre," Electron. Lett. **27**, 1785-1786 (1991).
3. J.E. Roman, P. Camy, M. Hempstead, W.S. Brocklesby, S. Nouth, A. Beguin, C. Lerminiaux, J. S. Wilkinson, "Ion-exchanged Er/Yb waveguide laser at 1.5 μm pumped by laser diode," Electron. Lett. **31,** 1345-1346 (1995).
4. A. Pollack and D.B. Chang, "Ion-pair upconversion pumped laser emission in Er^{3+} ions in YAG, YLF, SrF_2, and CaF_2 crystals," J. Appl. Phys. **64**, 2885-2893 (1988).
5. M.C. Nostrand, R.H. Page, S.A. Payne, W.F. Krupke, P. G. Schunemann, and L.I. Isaenko, "Spectroscopic data for infrared transitions in $CaGa_2S_4$:Dy^{3+} and KPb_2Cl_5: Dy^{3+}," OSA TOPS **19**, 524-528 (1998).
6. M.C. Nostrand, R.H. Page, S.A. Payne, W.F. Krupke, P. G. Schunemann, and L.I. Isaenko, "Room temperature $CaGa_2S_4$:Dy^{3+} laser action at 2.43 and 4.31 μm and KPb_2Cl_5: Dy^{3+} laser action at 2.43 μm," OSA TOPS **26**, 441-449 (1999).
7. M.C. Nostrand, R.H. Page, S.A. Payne, L.I. Isaenko, and A.P. Yelisseyev, "Optical properties of Dy^{3+}-and Nd^{3+}-doped KPb_2Cl_5," J. Opt. Soc. Am. B **18**, 264-276 (2001).
8. R. Balda, M. Voda, M. Al-Saleh, and J. Fernández, "Visible luminescence in KPb_2Cl_5:Pr^{3+} crystal," J. Lumin. **97**, 190-97 (2002).
9. A. Mendioroz, J. Fernández, M. Voda, M. Al-Saleh, R. Balda, and A. J. Garcia-Adeva, "Anti-Stokes laser cooling in Yb^{3+}-doped KPb_2Cl_5 crystal," Opt. Lett. **27**, 1525-1527 (2002).
10. N.W. Jenkins, S.R. Bowman, S.O´Connor, S.K. Searles, J. Ganem, "Spectroscopic characterization of Er-doped KPb_2Cl_5 laser crystal," Opt. Mat. **22**, 311-320 (2003).
11. R. Balda, J. Fernández, A. Mendioroz, M. Voda, and M. Al-Saleh, "Infrared-to-visible upconversion processes in Pr^{3+}/Yb^{3+}-codoped KPb_2Cl_5," Phys. Rev. B **68**, 1651011-1651017 (2003).
12. R. Balda, A. J. Garcia-Adeva, M. Voda, and J. Fernández, "Upconversion processes in Er^{3+}-doped KPb_2Cl_5," Phys. Rev. B **69**, 2052031-2052038 (2004).
13. M. Voda, M. Al-Saleh, R. Balda, J. Fernández, G. Lobera "Crystal Growth of Rare-earth-doped Ternary Potassium Lead Chloride Single Crystals by the Bridgman Method," Opt. Mat. **26**, 359-363 (2004).
14. K. Nitsch, M. Dusek, M. Nikl, K. Polák, and M. Rodová, "Ternary alkali lead chlorides: crystal growth, cristal structure, absorption and emission properties," Prog. Crystal Growth and Charact. **30**, 1-22 (1995).

#6367 - $15.00 US Received 19 January 2005; revised 11 March 2005; accepted 12 March 2005

15. R. Balda, J. Fernández, J.L. Adam, and M.A. Arriandiaga, "Time-resolved fluorescence-line narrowing and energy transfer studies in a Eu^{3+}-doped fluorophosphate glass," Phys. Rev. B **54**, 12076-12086 (1996).
16. G. Blasse, A. Bril, and W.C. Nieuwpoort, "On the Eu^{3+} fluorescence in mixed metal oxides. Part I- The crystal structure sensitivity of the intensity ratio of electric and magnetic dipole emission," J. Phys. Chem. Solids **27**, 1587-1592 (1966).
17. G. Blasse and A. Bril, "On the Eu^{3+} fluorescence in mixed metal oxides. II The $^5D_0 - {}^7F_0$ emission," Philips Res. Repts. **21**, 368-378 (1966).
18. W.C. Nieuwpoort and G. Blasse, "Linear Crystal-Field Terms and $^5D_0$–$^7F_0$ transition of Eu^{3+} ion," Sol. State Commun. **4**, 227-232 (1966).
19. C. Görller-Walrand and K. Binnemans, "Rationalization of Crystal-Field Parametrization", in *Handbook on the Physics and Chemistry of Rare Earths*, K.A. Gschneidner Jr. and L. Eyring, eds. (Elsevier Science, Amsterdam, 1996), vol.23 pp. 121-283.
20. B.G. Wybourne, *Spectroscopic Properties of Rare Earths*, Wiley, New York, 1965.
21. P. Porcher, Fortran routine GROMINET for simulation of real and complex crystal-field parameters on $4f^6$ and $4f^8$ configurations, (unpublished 1995).
22. S.V. Myagkota, A.S. Voloshinovskii, I.V. Stefanskii, M.S. Mikhalik, I.P. Pashuk, "Reflection and emission properties of lead-based perovskite-like crystals," Radiation Measurements **29**, 273-277 (1998).
23. L. Isaenko, A. Yelisseyev, A. Tkachuk, S. Ivanova, S. Vatnik, A. Merkulov, S. Payne, R. Page, M. Nostrand, "New laser crystal based on KPb_2Cl_5 for IR region," Mater. Science and Engineering **B81** 188-190 (2001).
24. Cotton and Wilkinson, *Advanced Inorganic Chemistry* (Wiley 1980).
25. P. Porcher, M. Couto dos Santos, and O. Malta, "Relationship between phenomenological crystal field parameters and the crystal structure: The simple overlap model," Phys. Chem. Chem. Phys. **1**, 397-405 (1999).

1. Introduction

Over the past few years, the interest in the search of rare earth (RE) doped low-energy phonon host materials has increased, specially for solid state upconversion lasers and mid-infrared lasers [1-4]. Hosts with low phonon energy lead to low non-radiative transition rates due to multiphonon relaxation and high radiative transition rates, which increase the quantum efficiency from excited states of active ions. Sulfide-and chloride-based hosts have been studied as their phonon energies are lower than those in the most extensively studied fluoride compounds. However, these materials usually present poor mechanical properties, moisture sensitivity, and are difficult to synthesize. Recently, potassium lead chloride, KPb_2Cl_5, has been studied as a promising host for RE ions [5-13] because it is non-hygroscopic and readily incorporates RE ions. The crystal is biaxial, crystallizes in the monoclinic system [14] and it is transparent in the 0.3 to 20 μm spectral region. According to Raman-scattering measurements [7] the maximum phonon energy, measured at the highest energy peak of the spectrum, is 203 cm^{-1}.

In RE doped KPb_2Cl_5 crystals the RE ions are supposed to substitute the lead (Pb^{2+}) ions whereas potassium (K^+) vacancies are assumed to provide charge compensation [7]. However, it is well established that the presence of structural defects in the vicinity of the RE ions may modify the local crystal-field symmetry and strength and may lead to a variety of nonequivalent RE optical centers. Unfortunately at this moment no accordance exists with respect to either the number of independent positions for Pb atoms or their coordination [7,10,14] . If there are various nonequivalent crystallographic sites for Pb^{2+} ion in the material lattice one could expect a rather complex spectroscopic behavior for the RE active ions. However, a recent spectroscopic characterization of Er^{3+} in KPb_2Cl_5 performed by Jenkins el al. [10] concluded that the erbium ion replaced only one of the two available non-equivalent lead ion sites. In order to understand the underlying reasons for this behaviour and to clarify the nature of the RE environments in potassium lead chloride-type crystals we have undertaken the study of the site-resolved luminescence of Eu^{3+} in KPb_2Cl_5 account taken of the adequacy of the dopant ion as a structural probe. Since $^5D_0$ state is nondegenerate under any symmetry, the structure of the $^5D_0 \rightarrow {}^7F_J$ emission is only determined by the splitting of the terminal levels caused by the local crystal field. Moreover, as the $^7F_0$ level is also

#6367 - $15.00 US Received 19 January 2005; revised 11 March 2005; accepted 12 March 2005

nondegenerate, site-selective excitation within the inhomogeneous broadened $^7F_0 \rightarrow {}^5D_0$ absorption band can be performed by using fluorescence line narrowing (FLN) technique to distinguish among different local environments around the rare-earth ions. On the ground of the experimental results a crystal-field analysis and simulation of the energy level schemes have also been performed in order to parametrize the crystal-field around the Eu^{3+} ions. As a conclusion, we found evidences about the existence of at least three symmetry independent crystal field sites for the RE ions in this crystal. A plausible argument about the crystallographic nature of these sites is finally given.

2. Experimental techniques

Single crystals of non-hygroscopic ternary potassium-lead chloride KPb_2Cl_5 doped with Eu^{3+} ions, typically 2 cm long and 1 cm in diameter, have been grown in our laboratory by the Bridgman technique, in a chlorine atmosphere, with a two-zone transparent furnace, a vertical temperature gradient of 18 ºC/cm, and a 1mm per hour growth rate. Quartz ampoules with a pointed end were used as seed selectors to promote single crystal growth. The pure crystals are transparent and colourless. The Eu^{3+} content was 0.5 mol % in the melt. The plates with approximate dimensions of 8x4x2 mm^3 were cut from blocks and polished for spectroscopic measurements.

Resonant time-resolved FLN spectra were performed by exciting the sample with a pulsed frequency doubled Nd:YAG pumped tunable dye laser of 9 ns pulsed width and 0.08 cm^{-1} linewidth and detected by an EGG&PAR Optical Multichannel Analyzer. The measurements were carried out by keeping the sample temperature at 10 K in a closed cycle helium cryostat.

For lifetime measurements, the fluorescence was analyzed with a 0.25 m Jobin-Ybon monochromator and the signal detected by a Hamamatsu R636 photomultiplier. Data were processed by a Tektronix oscilloscope.

3. Experimental results

3.1 FLN spectra

Time-resolved line-narrowed fluorescence spectra of the $^5D_0 \rightarrow {}^7F_{0\text{-}6}$ transitions of Eu^{3+} doped KPb_2Cl_5 crystal were obtained at 10 K by using different resonant excitation wavelengths into the $^7F_0 \rightarrow {}^5D_0$ transition, and at different time delays after the laser pulse. Depending on the excitation wavelength the emission spectra present very diverse characteristics, mainly regarding the number of observed $^5D_0 \rightarrow {}^7F_J$ transitions, their relative intensity and the magnitude of the observed crystal-field splitting for each ^7F_J state. As an example Fig. 1 shows the spectra corresponding to the $^5D_0 \rightarrow {}^7F_{0,1,2}$ transitions obtained with a time delay of 10 μs after the pump pulse at four different pumping wavelengths. At the lowest excitation wavelength, 578.5 nm, the $^5D_0 \rightarrow {}^7F_0$ transition shows the presence of at least three resolved peaks which indicates the existence of different RE sites. Indeed, the $^5D_0 \rightarrow {}^7F_{0,1,2}$ spectra obtained by exciting at 579.5, 580.1, and 581 nm respectively, selectively show the presence of the three isolated Eu^{3+} sites.

We shall hereafter refer to the optical features of these spectra as originating from sites I (λ_{exc} = 579.5 nm), II (λ_{exc} = 580.1 nm) and III (λ_{exc}= 581 nm). On the other hand, while tuning the excitation pulse at other wavelengths the observed spectra consist of overlapped series of peaks corresponding to the three sites. The presence of the line for the $^5D_0 \rightarrow {}^7F_0$ transition in each spectrum indicates a site of C_{nv}, C_n or C_s symmetry for Eu^{3+}. These symmetries allow the transition as an electric dipole process, according to the group theory selection rules, with a linear term in the crystal-field expansion [16-18]. By making use of the selection rules for induced electric dipole (ED) and magnetic dipole (MD) transitions, that is, from the comparison between the derived number of possible and experimentally observed $^5D_0 \rightarrow {}^7F_{0\text{-}6}$ transitions, it is in principle likely to discriminate between different symmetry point groups for these Eu^{3+} optical centers [19].

#6367 - $15.00 US Received 19 January 2005; revised 11 March 2005; accepted 12 March 2005

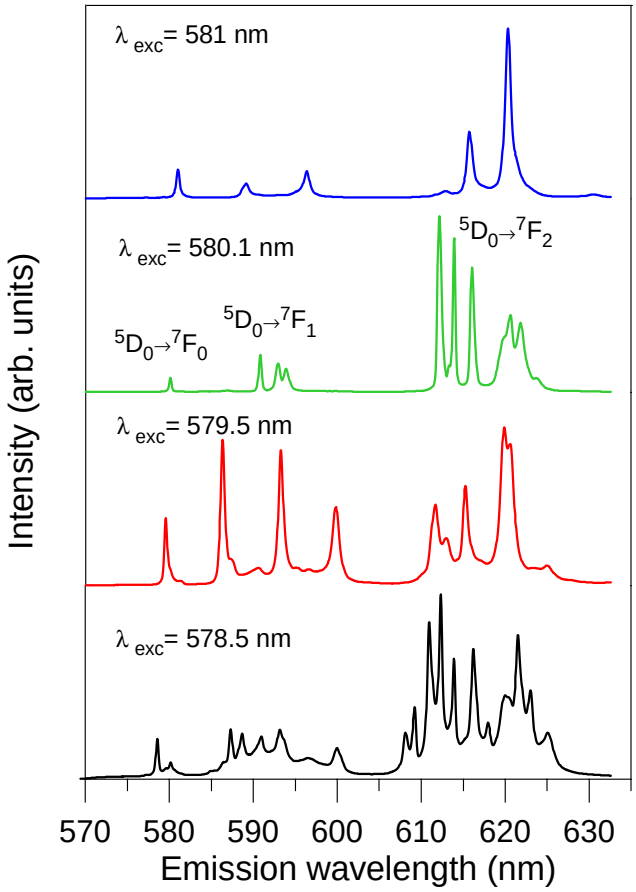

Fig. 1. $^5D_0 \rightarrow F_{0,1,2}$ emissions of Eu^{3+} in KPb_2Cl_5

In this way, the spectra obtained with excitation wavelengths 579.5 and 580.1 nm display, in both cases, three Stark levels for the $^5D_0 \rightarrow ^7F_1$ transition and five levels in the hypersensitive $^5D_0 \rightarrow ^7F_2$ region, meaning that the degeneracy of these two states is completely lifted, that is, I and II Eu^{3+} optical centers are located in crystal sites with C_{2v} or lower symmetry. These levels as well as those observed for remaining transitions from $^5D_0$ to the ground ^7F_J manifold are included in Table 1 (shown in the Appendix). However, the noticeably different patterns observed when comparing the fluorescence spectra from I and II sites indicate very distinct Eu^{3+} crystalline environments. As can be observed in Fig. 1, the intensity ratio of the $^5D_0 \rightarrow ^7F_1$ and $^5D_0 \rightarrow ^7F_2$ emissions is about one for site I, whereas the relationship is reduced to about one third for site II. Regarding the rest of the $^5D_0 \rightarrow ^7F_J$ transitions, shown in Fig. 2, it is also surprising to find the very low intensity of the $^5D_0 \rightarrow ^7F_3$ transition detected at excitation wavelength 580.1 nm. This transition, forbidden in first order by the electric/magnetic dipole selection rules, is observed only as a consequence of the J-mixing, which mixes the $^7F_3$ wavefunctions with other ^7F_J ones, through the second- and fourth-order crystal-field (CF) parameters. Finally, the quite large observed splitting of $^7F_1$ for site I, 382 cm^{-1}, clearly contrasts with the corresponding to site II, of about 87 cm^{-1}.

#6367 - $15.00 US Received 19 January 2005; revised 11 March 2005; accepted 12 March 2005

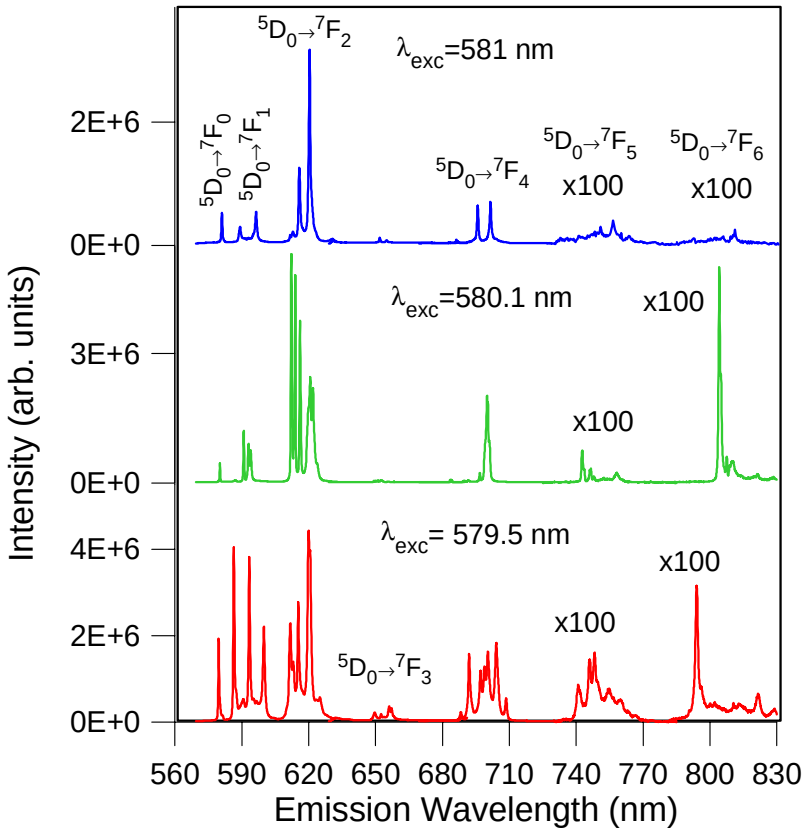

Fig. 2 . $^5D_0 \rightarrow F_{0\rightarrow 6}$ emissions of Eu^{3+} in KPb_2Cl_5

On the other hand, the spectra obtained by exciting at 581 nm only show two CF levels for the $^5D_0 \rightarrow {}^7F_1$ transition, and three levels (one of them with a very weak intensity) for the $^5D_0 \rightarrow {}^7F_2$ emission. These results suggest that Eu^{3+} in site III is in the presence of a rather higher hexagonal, trigonal or tetragonal symmetry. A careful analysis of the whole set of levels from $^5D_0 \rightarrow {}^7F_J$ transitions clearly allows to exclude higher hexagonal D_6, C_{6v},C_6, D_{3h}, and C_{3h} symmetries, as well as tetragonal D_4, for which the number of energy levels to be likely observed would be lesser than in the identified set, whereas tetragonal C_{4v}, D_{2d}, S_4 and C_4, and trigonal C_{3v}, D_3 and C_3 symmetries seem to be a better approach and deserve a more detailed evaluation. The results corresponding to attempts of parametrization of CF effects for Eu^{3+} located in site III developed on the basis of local C_{4v} and C_{3v} or D_3 symmetries are presented in Table 2 (shown in the Appendix).

3.2 Lifetimes

As could be expected, if there are different sites for the Eu^{3+} ion, the lifetime of state $^5D_0$ should depend on the excitation wavelengths. We have measured the lifetime of the $^5D_0$ state at three different excitation wavelengths (579.5, 580.1, and 581 nm), which correspond to those at which the three sites are selectively resolved, and collecting the luminescence at the highest intensity Stark component of the $^5D_0 \rightarrow {}^7F_4$ transition. The experimental decays are well described by a single exponential function to a good approximation. The values of the measured lifetime are 1.1 ms, 0.55 ms, and 0.14 ms for sites I, II, and III respectively.

#6367 - $15.00 US Received 19 January 2005; revised 11 March 2005; accepted 12 March 2005

4. Crystal-field analysis and simulation of the energy level schemes

It is well known that Eu^{3+} is the best choice for a 'crystal-field probe' in a given host. Their ground $^7F_0$ as well as the fluorescent $^5D_0$ states are non-degenerate, and have symmetry label Γ_1, which largely simplifies the interpretation of the spectra. By making use of the selection rules for induced ED and MD transitions, it is possible to discriminate between different point symmetries for an observed optical center in a given host. Moreover, there is a straightforward relation between the CF splitting of $^{2S+1}L_J$ levels with small J values, especially for J = 1 and 2, and the CF parameters. In this case, CF parameters can be deduced directly from the experiment.

The phenomenological CF simulation of the Eu^{3+} energy level scheme can be accurately conducted on the strongly reduced basis of the $^7F_{JM}$ set alone, i.e., 49 $|\, SLJM_J\rangle$ levels. The use of this truncation is enabled by two characteristics of the $4f^6$ configuration: firstly, the ^7F_J (J = 0 - 6) sextuplet is relatively well isolated from the rest of the configuration (the energy gap between $^7F_6$ and $^5D_0$ is ~12 000 cm^{-1}), which renders the mixing of the wavefunctions negligible, and secondly, the CF operator only mixes levels with the same multiplicity. Evidently, even with the J-mixing included, not all the interactions are taken into account, as non-diagonal spin-orbit interactions that create small components of the ^5D_J levels into the ^7F_J wavefunctions. Therefore, some "intermediate parameters" have to be introduced, one for each ^7F_J state, in order to overlap experimental and calculated barycenters.

The method used for calculating the energy levels of Eu^{3+} in a crystalline environment usually considers the single-particle CF theory. Following the formalism of Wybourne [20], the CF Hamiltonian is expressed as a sum of products of tensor operators $(C_q^k)_i$, with real B_q^k and complex S_q^k parameters as coefficients, these later appropriated to the Eu^{3+} site symmetry in the host

$$H_{CF} = \sum_{k=2}^{4,6} \sum_{q=0}^{k} \left[B_q^k (C_q^k + (-1)^q C_{-q}^k) + i S_q^k (C_q^k - (-1)^q C_{-q}^k) \right]$$

For I and II Eu^{3+} sites in KPb_2Cl_5, which in accordance with the above fluorescence spectra present C_{2v} or lower symmetries, we have carried out the parametrization by initially considering the nine real B_q^k parameters of a C_{2v} CF potential. Secondly, fourth and sixth-rank parameters were carefully determined from the adequate reproduction of $^7F_1$, $^7F_2$ and the remaining observed ^7F_J splittings, respectively, before considering all observed energy levels and a free variation of all CF parameters. Thirty energy levels for site I and thirty three ones for site II, included in Table 1, were used to derive these parameters. The phenomenological sets of refined C_{2v} parameters for sites I and II are presented in Table 2. After this first step, the preceding nine CF parameters can be considered as the starting ones for the simulation of the same energy level patterns in the lower C_s/C_2 symmetry, which involves the corresponding non-zero complex S_q^k parameters. The results are included in Table 2.

A scheme of 18 Stark levels was considered for the simulation of the sequence of Eu^{3+} ^7F_J energy levels in site III, when the C_{4v} symmetry is evaluated. Two more levels, which were seen from weak transitions, were added for the simulation with the C_{3v} or D_3 symmetry, Table 1. Results of refined CF parameters for both fittings C_{4v} and C_{3v}/D_3 are included in Table 2. All the performed calculations were conducted with the aid of a matrix diagonalizing program [21] which took into account the J mixing between wavefunctions with different J and M values. The least squares refinement between the experimental and calculated energy levels was carried out by minimizing the rms function defined as $\sigma = \left[\sum \left(E_{\exp} - E_{cal} \right)^2 / \left(N_{lev} - N_{par} \right) \right]^{1/2}$, where E_{exp} and E_{cal} correspond to the experimental

#6367 - $15.00 US Received 19 January 2005; revised 11 March 2005; accepted 12 March 2005

and calculated energy level values, and N_{lev} and N_{par} the number of levels and parameters, respectively. Figure 3 shows the observed and calculated energy levels for the three sites.

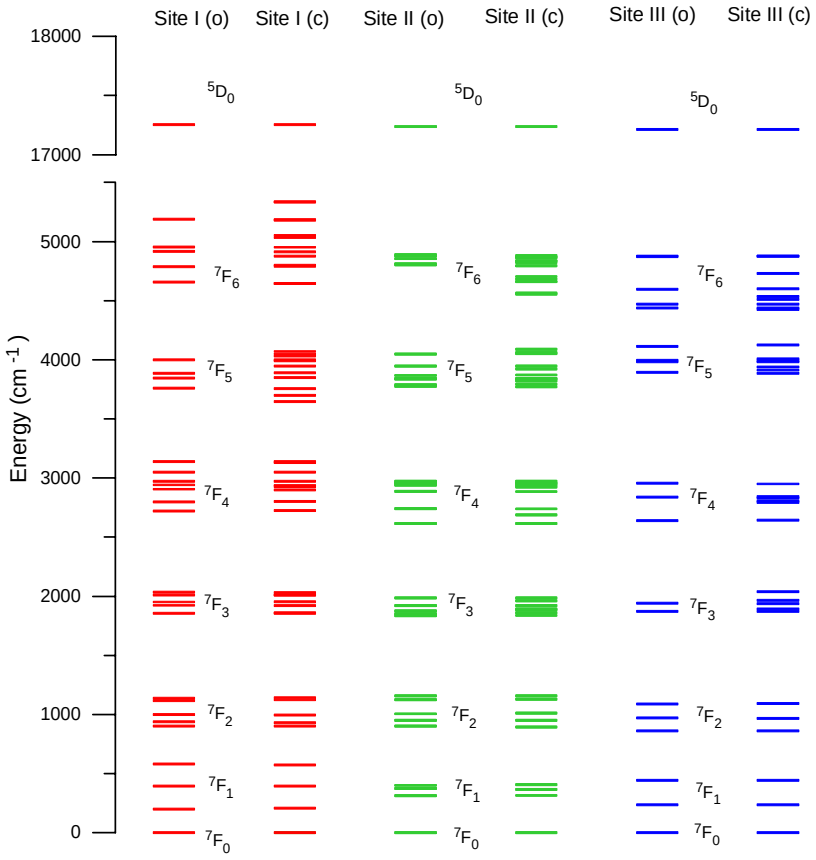

Fig.3. Observed (o) and calculated (c) energy levels for the three Eu^{3+} sites

5. Discussion

The existence of diverse Eu^{3+} optical centers must be explained on the basis of the crystal structure of the KPb_2Cl_5 host in which they are embedded, that is, three different crystallographic sites for Eu^{3+} in europium-doped KPb_2Cl_5 crystal must be assumed.

According to X-ray analysis, biaxial crystals KPb_2Cl_5 present the monoclinic symmetry of the space-group $P2_1/c$, with lattice parameters (Å) a = 8.831(2), b = 7.886(2) and c = 12.430(3), β = 90.14 (2)°, V = 865.6(4) and Z = 4 [14]. The β value near 90 ° indicates that the crystal is nearly orthorhombic. Although all studies on the crystal structure of KPb_2Cl_5 reveal that the $[PbCl_6]^{4-}$ distorted octahedron is a principal element, no accordance exists with respect to either the number of independent positions for Pb atoms or their coordination. Thus, while some authors report the existence of four non-equivalent Pb sites, [7,22] others point to Pb occupying two symmetrically independent positions [14]. In this last case, the Pb(1) coordination can be described as a distorted mono-capped octahedron (coordination number CN=7), with the seventh apex at distance > 3.1 Å, and Pb(2) is located in the center of a tri-capped trigonal prism of chlorine atoms (CN=9), where one of the capping ligands is at the large distance ~ 4.2 Å, [14] being thus more reasonable to regard this Pb(2) coordination polyhedron as a bi-capped trigonal prism (CN=8) of chlorine atoms. Anyway, if a smaller

#6367 - $15.00 US Received 19 January 2005; revised 11 March 2005; accepted 12 March 2005

coordination sphere around Pb atoms is considered, Pb(1) will be in a purely octahedral environment, CN=6, with Pb-Cl distances < 3Å, and Pb(2) possesses an umbrella-like environment with two other more remote Cl^-, at around 3.2 Å, and then CN=7 [23].

The distribution of chlorine atoms around K corresponds to a tricapped trigonal prism TTP (CN=9), where one of the equatorial capping atoms is at distance ~ 3.8 Å. Figure 4 shows the coordination polyhedra around Pb(1) (CN=7), Pb(2) (CN=9) and K (CN=9) respectively, in KPb_2Cl_5.

Eu^{3+} ions are supposed to substitute Pb^{2+} in the above positions, and the charge compensation will be ensured by K^+ vacancies. However taking into account that the K^+ coordination polyhedron is similar to the one described for Pb(2), and that actually the planes occupied by Pb^{2+} and K^+ ions alternate within the framework [14], the possibility of a further Eu^{3+} access to K^+ sites should be also considered though it would suppose a hardly stable local distribution in the crystal host requiring a nearby Pb^{2+} vacancy for charge compensation.

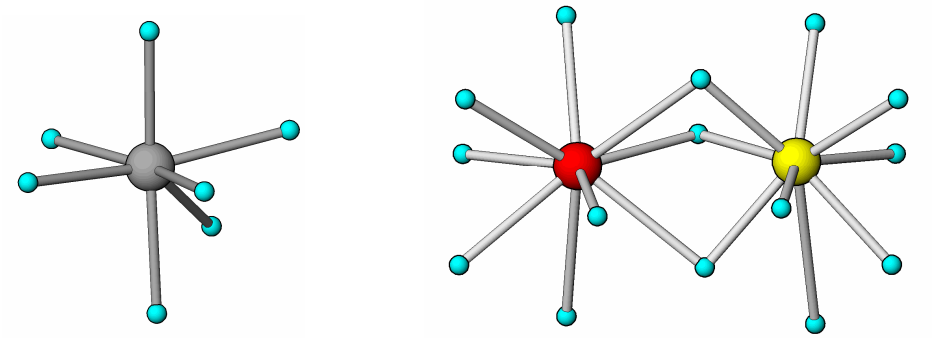

Fig. 4. Coordination polyhedra of Pb and K in KPb_2Cl_5. Their site symmetries are Pb(1) = C_2/C_s, K = D_3/C_{3v}, and Pb(2) ~ C_{2v}. Grey, red, yellow, and blue balls represent Pb(1), K, Pb(2), and Cl atoms, respectively. Crystal data were derived from Ref. 14.

Simulations of spectra for Eu^{3+} located in C_{2v} I and II sites yielded energy levels schemes in very good agreement with the experimental data. They were, however, undoubtedly improved when the complex S_q^k parameters of the symmetry C_2/C_s were introduced, since σ deviations as well as residues decreased significantly. Anyway, complex CF parameters for site II are really weaker, with values of only a few cm^{-1}, and this suggests that the deviation from the higher C_{2v} is, in this case, negligible. By the contrary, results from the fit under C_2/C_s symmetry for site I reveal rather important values for complex S_q^k parameters, mainly for sixth-rank ones. Consequently, it seems that site I is far more distorted than site II from the initially considered C_{2v} symmetry.

On the other hand, independently of the symmetry considered, the second-order CF parameters for site II are always small, and consequently the J-mixing through the $^7F_1$ wavefunctions will be also small, which explains the above indicated low intensity for the $^5D_0 \rightarrow {}^7F_3$ transition.

Finally, the important difference between absolute values of B_0^2 and B_2^2 parameters for each site reflects the considerably different splitting of their corresponding $^7F_1$ levels.

From results of the CF analysis for Eu^{3+} in site III it is clear that it is consistent with a local environment related to a TTP coordination polyhedron CN=9, that is adopted by K^+ cations in KPb_2Cl_5. However, the full corresponding D_{3h} symmetry, described only by parameters B_0^2, B_0^4, B_0^6 and B_6^6 is not retained. If in TTP a twist for both top and base relative to each other over a distortion angle occurs, the symmetry is lowered first to D_{3h}, and

#6367 - $15.00 US Received 19 January 2005; revised 11 March 2005; accepted 12 March 2005

finally to D_3 appearing two additional CF parameters, B_3^4 and B_3^6, as it is currently derived from our CF analysis. On the other hand, the D_{3h} symmetry is lowered to C_{3v} if the three capping ligands are removed out of the equatorial plane, but all in the same direction and with the same distortion angle. The C_{3v} potential is described by the same set of CF parameters than D_3. It is worthy to consider that account taken of the crystallographic coordination polyhedron around K^+ (CN=9) mentioned above (see Fig.4) a most realistic symmetry for site III could be C_3.

Finally, some additional insight about the crystallographic nature of Eu^{3+} sites can be obtained from the measured lifetimes. As we have seen, the longest lifetime, 1.1 ms, corresponds to site I whose abundance, as estimated from the emission of the ED $^5D_0 \rightarrow {}^7F_2$ transition, is only a 2 % of the one corresponding to site II. The less ED character of this transition if compared with the other RE sites suggests a less distorted ligand symmetry around the RE ion but, at the same time, the large Stark splitting of the $^7F_1$ components (Fig. 1) indicates a stronger CF which could arise from shorter RE-Cl bond distances expected at this site [14] (see Fig. 4). Paying attention to these points, one could guess Pb(1) crystallographic site as a probable candidate for the Eu^{3+} (I) site. On the other hand, the lifetime of $^5D_0$ state of Eu^{3+} in site II (the more abundant one), 0.55 ms, agrees well with the more distorted ligand symmetry related to Pb(2) crystallographic sites (see Fig.4) which is in accordance with a more ED character shown by the $^5D_0 \rightarrow {}^7F_2$ transition. For both Pb sites, the charge compensation can be easily attained by K^+ vacancies. Finally, the unexpected relatively high CF symmetry of Eu^{3+} in CF site III (abundance 1.2 % referred to site II) contrasts with the shortest lifetime of the $^5D_0$ state in this matrix. Account taken of the crystallographic information shown in Fig. 4 one could suggest the crystallographic site of K^+ ion as a rather possible place for Eu^{3+} in CF site III. Indeed, the ligand local environment is related to a TTP coordination polyhedron which has enough room for the RE and could display the required C_3 symmetry. On the other hand, the short lifetime of the $^5D_0$ state agrees well with the strong splitting of the $^7F_1$ components and the pronounced ED character of the $^5D_0 \rightarrow {}^7F_2$ transition which suggest a still remarkable CF distortion of the ligands promoted by the nearby Pb(2) vacancy needed for the charge compensation.

To further assess the likeliness of current phenomenological parametrizations of crystal field (CF) effects for the three Eu^{3+} crystal sites resolved in KPb_2Cl_5, we have also carried out semi-empirical simulations of the CF features observed. They have been conducted through the Simple Overlap Model (SOM) for the crystal field [25]. Benefiting from the fact that the SOM model uses the crystallographic positions of the $Eu(Pb1)Cl_7$, $Eu(Pb2)Cl_9$ and $Eu(K)Cl_9$ coordination polyhedra in the estimation of CF parameters, these calculations have supposed some little modifications ($\pm$ 10 %) in Eu (in Pb(1), Pb(2) and K sites) - Cl distances, with regards to those in Ref. 14. These atom displacements are needed to account for distortions induced in the actual KPb_2Cl_5 host, which arise from the existence of Pb vacancies necessary for charge compensation. Table 3 (shown in the Appendix) summarizes the main FLN experimental results together with the relationship between the second order calculated crystal field parameters and the ones simulated by using the crystallographic coordinates of the nearest ligands at the proposed lattice sites occupied by the Eu^{3+} ion.

In summary, if we take into account the proclivity of lanthanide ions for CN=9 within a more or less distorted tricapped trigonal prism [24] and that Pb vacancies are rather difficult to achieve in the KPb_2Cl_5 due to the framework, we can easily understand why Eu^{3+} in site Pb(2) is the more abundant one, nearly 97% in potassium lead chloride crystal.

6. Conclusion

By using fluorescence line narrowing technique we have demonstrated the existence of three different local environments around the RE ions in KPb_2Cl_5. On the ground of the experimental results, the crystal-field analysis and simulation of the energy level schemes allow to connect the predicted symmetry of the resolved sites with the crystal structure. In

#6367 - $15.00 US Received 19 January 2005; revised 11 March 2005; accepted 12 March 2005

conclusion, the RE ions may occupy both the Pb and K sites but the luminescence results suggest that RE ions occupying the Pb(2) site is most likely to occur.

Acknowledgments

This work was supported by the Spanish Government MEC (MAT2004-03780 and MAT2004-02001) and Basque Country University (UPV13525/2001).

Appendix

Table 1. Observed and calculated energy levels (cm^{-1}) of observed Eu^{3+} optical centers in KPb_2Cl_5

	Site I		Site II		Site III	
	C_2/Cs		C_2/Cs		D_3/C_{3v}	
$^{2S+1}L_J$	Eo	Ec	Eo	Ec	Eo	Ec
^7F_o	0.1	0.1	0.1	0.1	0.1	0.1
$^7F_1$	198.6	208.2	312.8	315.3	237.8	236.8
	392.6	394.2	372.4	365.7	442.1	443.0
	580.4	572.5	400.4	405.3		
$^7F_2$	902.7	902.3	903.0	894.3	860.1	862.2
	938.4	930.3	950.1	951.1	969.3	965.7
	998.4	994.4	1005.9	1010.6	1090.3	1092.2
	1118.7	1122.7	1125.7	1128.2		
	1136.9	1142.5	1157.0	1157.8		
$^7F_3$	1855.8	1857.4	1836.8	1837.5	1870.6	1872.6
	-	1860.3	1852.7	1860.8	-	1891.9
	1923.0	1918.7	1877.3	1882.9	1939.2	1938.0
	1951.4	1953.3	-	1893.4	-	1964.6
	2008.0	2009.2	1918.7	1920.5	-	2037.9
	-	2009.5	-	1960.8		
	2033.7	2029.7	1986.2	1985.5		
$^7F_4$	2721.7	2723.4	2614.5	2615.8	2638.4	2642.1
	2799.1	2801.9	-	2688.0	-	2792.1
	2905.4	2898.8	2739.8	2738.7	-	2805.7
	-	2926.4	2885.7	2885.4	-	2829.5
	2941.4	2937.5	-	2922.8	2839.2	2842.7
	2973.3	2971.0	2937.4	2937.9	2956.2	2949.8
	3049.4	3050.5	2952.9	2952.9		
	-	3129.5	2959.6	2957.9		
	3138.3	3138.8	2971.9	2972.0		
$^7F_5$	-	3648.6	3775.4	3770.4	3893.4	3886.8
	-	3699.0	3788.5	3792.0	-	3913.6
	3759.4	3756.6	-	3819.7	-	3939.1
	3847.4	3849.6	3837.1	3836.2	3982.7	3982.0
	3887.4	3890.9	3843.6	3843.1	3995.5	3993.0
	-	3946.2	3868.1	3872.0	-	4007.8
	-	3991.7	-	3923.4	4115.1	4124.4
	4000.3	3998.9	3948.3	3947.2		
	-	4034.0	4049.2	4051.6		
	-	4050.9		4061.3		
	-	4071.1		4089.0		
$^7F_6$	-	4645.9	-	4557.1	-	4427.0
	4657.3	4646.9	-	4563.3	4438.3	4437.2
	4787.1	4791.1	-	4660.1	4470.7	4470.6
	-	4801.3	-	4663.4	-	4509.9
	-	4878.1	-	4683.7	-	4537.8
	4915.9	4912.5	-	4704.4	4598.0	4602.6
	4954.5	4952.1	4803.2	4794.3	-	4729.9
	-	5033.7	4814.2	4821.7	4874.1	4875.8
	-	5051.8	-	4838.1	4879.6	4875.9
	-	5182.2	4855.0	4865.0		
	5189.6	5183.7	-	4867.4		
	-	5334.2	4875.0	4873.7		
	-	5334.3	4888.5	4880.6		

#6367 - $15.00 US Received 19 January 2005; revised 11 March 2005; accepted 12 March 2005

Table 2. Phenomenological crystal-field parameters (cm^{-1}) for observed Eu^{3+} optical centers in KPb_2Cl_5

	Site I		Site II			Site III			
	C_{2v}	C_s/C_2		C_{2v}	C_s/C_2		C_{4v}		C_{3v}
B_0^2	-1019(14)	-1022(14)	B_0^2	170(17)	189(16)	B_0^2	-783(19)	B_0^2	730(10)
B_2^2	-396(11)	-392(11)	B_2^2	91(12)	85(12)		-		
B_0^4	-187(31)	-232(29)	B_0^4	232(36)	150(36)	B_0^4	-820(36)	B_0^4	-547(23)
B_2^4	-358(28)	-313(29)	B_2^4	1184(14)	1159(14)		-		
S_2^4	-	-110(36)	S_2^4	-	23(32)		-	B_3^4	461(22)
B_4^4	314(21)	307(27)	B_4^4	278(20)	306(19)	B_4^4	626(32)		
S_4^4	-	-21(34)	S_4^4	-	32(31)		-		
B_0^6	-379(34)	-408(37)	B_0^6	-730(39)	-876(34)	B_0^6	584(59)	B_0^6	809(26)
B_2^6	-200(28)	-196(29)	B_2^6	48(22)	32(22)		-		
S_2^6	-	97(47)	S_2^6	-	-148(32)		-	B_3^6	-254(34)
B_4^6	-954(26)	-658(30)	B_4^6	121(25)	78(30)	B_4^6	510(37)		
S_4^6	-	-690(42)	S_4^6	-	2(46)		-		
B_6^6	515(25)	358(31)	B_6^6	-227(25)	-226(29)			B_6^6	8(34)
S_6^6	-	405(35)	S_6^6	-	47(38)		-		
levels	30	30	levels	33	33	levels	18	levels	20
d_m	5.8	4.5	d_m	5.5	4.4	d_m	7.9	d_m	3.7
σ	6.9	6.2	σ	6.4	5.5	σ	9.3	σ	4.4
R	1011.1	612.9	R	986.6	644.9	R	1120.9	R	270.8

#6367 - $15.00 US Received 19 January 2005; revised 11 March 2005; accepted 12 March 2005

Table 3. Summary of spectroscopic results and crystal field calculation and simulation

Site	FLN spectra	Phenomenological Crystal Field (CF) analysis	CF simulation based on Metal-Ligand (M-L) crystallographic distances
I	*Degeneracy for $^7F_1$ and $^7F_2$ levels*: Fully removed, 3 and 5 energy levels respectively *Expected symmetry:* C_{2v} or lower *Intensity ratio:* $^5D_0 \rightarrow {}^7F_1/{}^5D_0 \rightarrow {}^7F_2 \approx 1/1$ *Lifetime* ($^5D_0$): 1.1 ms	*Short range parameters* B_q^2 (cm^{-1}): -1022(14), -392 (11) *Derived symmetry*: C_2/C_s	*Short range parameters* B_q^2 (cm^{-1}): -1054, -364 *Derived symmetry*: C_2/C_s *Crystallographic assignment*: Eu^{3+} in Pb(1) site
II	*Degeneracy for $^7F_1$ and $^7F_2$ levels*: Fully removed, 3 and 5 energy levels respectively *Expected symmetry:* C_{2v} or lower *Intensity ratio*: $^5D_0 \rightarrow {}^7F_1/{}^5D_0 \rightarrow {}^7F_2 \approx 1/3$ Lifetime ($^5D_0$): 0.55 ms	*Short range parameters* B_q^2 (cm^{-1}): 189(16), 85(12) *Derived symmetry*: ~C_{2v}	*Short range parameters* B_q^2 (cm^{-1}): 185, 73 *Derived symmetry*: ~C_{2v} *Crystallographic assignment*: Eu^{3+} in Pb(2) site
III	*Degeneracy for $^7F_1$ and $^7F_2$ levels*: 2 and 3 energy levels respectively *Expected symmetry:* C_{4v}, D_3, C_{3v} *Intensity ratio* $^5D_0 \rightarrow {}^7F_1/{}^5D_0 \rightarrow {}^7F_2 \approx 1/3$ *Lifetime* ($^5D_0$): 0.14 ms	*Short range parameters* B_q^2 (cm^{-1}): 730(10) *Derived symmetry:* Compatible with C_{3v} and C_3	*Short range parameters* B_q^2 (cm^{-1}): 728 *Derived symmetry:* Compatible with C_{3v} and C_3 *Crystallographic assignment*: Eu^{3+} in K site

#6367 - $15.00 US Received 19 January 2005; revised 11 March 2005; accepted 12 March 2005